Physica B 407 (2012) 2974–2977

Contents lists available at ScienceDirect

Physica B

journal homepage: www.elsevier.com/locate/physb

Reconfigurations and diffusion of trivacancy in silicon

V.P. Markevich [a,*], A.R. Peaker [a], B. Hamilton [a], S.B. Lastovskii [b], L.I. Murin [b], J. Coutinho [c], A.V. Markevich [c], M.J. Rayson [d], P.R. Briddon [e], B.G. Svensson [f]

[a] Photon Science Institute, University of Manchester, Manchester M13 9PL, United Kingdom
[b] Scientific-Practical Materials Research Center of NAS of Belarus, Minsk 220072, Belarus
[c] I3N, Department of Physics, University of Aveiro, 3810-193 Aveiro, Portugal
[d] Department of Mathematics, Luleå University of Technology, Luleå S-97187, Sweden
[e] School of Electrical, Electronic and Computer Engineering, University of Newcastle upon Tyne, Newcastle NE1 7RU, United Kingdom
[f] Department of Physics, Oslo University, 0316 Oslo, Norway

ARTICLE INFO

Available online 5 August 2011

Keywords:
Silicon
Trivacancy
Diffusion
DLTS
ab-initio modeling

ABSTRACT

Disappearance of the divacancy (V_2) and trivacancy (V_3) complexes upon isochronal and isothermal annealing of electron irradiated Si:O crystals has been studied by means of deep level transient spectroscopy. The annealing studies have shown that the V_2 and V_3 defects are mobile in Si at $T > 200$ °C and in oxygen-rich material are trapped by interstitial oxygen atoms so resulting in the appearance of V_2O and V_3O defects. The activation energies for diffusion of the V_2 and V_3 centers have been determined. Density functional modeling calculations have been carried out to investigate the migration and reorientation mechanisms of V_3 in large silicon supercells. It is proposed that these comprise a sequence of transformations between $V_3(D_3)$ and $V_3(C_{2v})$ configurations.

1. Introduction

Vacancy-related clusters (V_n) in silicon are technologically important defects because of their role in capturing unwanted impurities and silicon self-interstitials so reducing enhanced diffusion of dopants in extremely scaled integrated circuits and silicon nanodevices. Such clusters have attracted a great attention recently (e.g., Refs. [1–3]).

Early density-functional theory (DFT) and Hatree–Fock calculations by Hastings and Estreicher [4] indicated that the lowest energy structures for small vacancy clusters were those obtained by sequential removal of host atoms from the hexagonal ring in the Si lattice. These are referred as part of hexagonal ring (PHR) structures, and the main argument behind their stability was the minimization of dangling bonds in such defects. However, based on similar dangling bond minimization arguments, recent DFT studies by Makhov and Lewis [1] have suggested that more stable structures can be obtained for the V_5, V_4 and V_3 complexes by successive passivation of up to three groups of four dangling bonds in a hexavacancy by placing one, two and three extra Si atoms, respectively, at stable sites edging the V_6 defect (see Fig. 1 of Ref. [1]). These complexes comprise a family of four-fold coordinated (FFC) vacancy defects. Available experimental data on the transformations and diffusion of small V_n clusters with $n > 2$ is very limited (see e.g., Ref. [3] and references therein). Apart from a calculation of a minute 0.02 eV transformation barrier between FFC and PHR forms of V_5, there are no results of analogous calculations for other vacancy clusters, and the migration of the clusters has not been addressed by calculations at all. In the present work the results of a combined deep level transient spectroscopy (DLTS) and ab-initio modeling study on reorientation and migration of the V_3 complex are reported.

2. Experimental and modeling details

Experimental results in the present work were obtained by means of DLTS and high-resolution Laplace DLTS. One set of p^+–n–n^+ diodes and two sets of n^+–p–p^+ diodes were prepared for the study. p^+–n–n^+ diodes were formed by implantation and subsequent thermal activation of boron ions into phosphorus-doped ($\rho \approx 30\,\Omega$ cm) epi-Si grown on highly Sb-doped bulk Czochralski-grown (Cz) Si wafers. One set of n^+–p–p^+ diodes was produced on boron-doped epi-Si ($\rho \approx 20\,\Omega$ cm), which was grown on highly boron-doped Cz–Si wafers. The diodes were formed by implantation of phosphorus ions with subsequent annealing at 1150 °C in nitrogen–oxygen gas ambient. Oxygen concentrations in the epi-layers were estimated from the rate of transformation of V_2 to the divacancy-oxygen defect with the use of data presented in Ref. [5]. The oxygen concentration was close

* Correspondence to: School of Electrical and Electronic Engineering, University of Manchester, Sackville Str. Building, Manchester M13 9PL, United Kingdom. Tel.: +44 161 3064746; fax: +44 161 3064770.
E-mail address: V.Markevich@manchester.ac.uk (V.P. Markevich).

0921-4526/$ - see front matter © 2011 Elsevier B.V. All rights reserved.
doi:10.1016/j.physb.2011.08.001

to 4×10^{17} cm^{-3} in all the epi-Si samples. n^+–p–p^+ diodes from another set were prepared by phosphorus diffusion at about 1000 °C from PCl_3 gas ambient into a boron-doped ($\rho\approx5\ \Omega$ cm) Cz-Si wafer with an oxygen content of about 7.5×10^{17} cm^{-3}. The back side of the wafer was boron implanted followed by laser annealing in order to create a p^+ layer for contacting.

All the samples were irradiated with 6 MeV electrons at room temperature using a linear accelerator. The flux of electrons was 1×10^{12} cm^{-2} s^{-1}. Thermal anneals of the irradiated structures were carried out in a furnace in a dry N_2 ambient.

Electronic structure calculations were carried out using a density-functional code (AIMPRO) [6], along with the local spin density approximation (LSDA) for the exchange correlation potential [7]. Si 1s, 2s and 2p core states were accounted for by fully separable dual-space pseudopotentials [8], whereas valence states, i.e., Kohn–Sham eigenstates, were expressed as linear combinations of Cartesian–Gaussian atom centered functions with angular momentum up to $l=2$. Accordingly, all Si atoms were assigned with 8 sp basis functions plus 5 d-type polarization functions. Potential terms and charge density were Fourier transformed using a plane-wave basis set with an energy cut-off set at $E_{cut}=80$ Ry.

The host crystal was accounted for using 512-atom cubic supercells, from which three atoms were removed to produce a trivacancy center. All atoms are allowed to move along their forces during a conjugate gradient atomic relaxation cycle to minimize the energy. This was carried out until total energy and atom position changes dropped below 0.3 meV and 5×10^{-5} Å, respectively. The Brillouin zone was sampled at $\mathbf{k}=\Gamma$, and under these conditions, the equilibrium lattice parameter and bulk modulus are $a_0=5.3947$ Å and $B=98.3$ GPa, whereas the indirect Kohn–Sham energy gap and total energy gap are $\varepsilon_g=0.56$ eV and $E_g=A_e-I_e=1.33$ eV. Here A_e and I_e stand for the electron affinity and ionization potential, respectively, calculated from 512-atom bulk charged supercells (compensated by an uniform background charge of opposite sign).

Migration/transformation paths were investigated with the help of an improved Nudged Elastic Band (NEB) method [9]. As a starting point, a series of intermediate structures are linearly interpolated between the initial and final configurations, with each pair of consecutive structures being coupled by a virtual elastic band. While the elastic band introduces a penalty for too small or too large distances between neighboring structures, it brings them into contact with the minimum energy path connecting initial and final states (see Refs. [10, 11].

3. Experimental and modeling results and discussion

3.1. Experimental results

We will first summarize briefly the results obtained recently on the structure and electronic properties of the trivacancy in silicon [3,12]. It was shown that the V_3 defect is a bistable center in the neutral charge state, with a four-fold coordinated (FFC) configuration lower in energy than the (1 1 0) planar one [3]. However, the (1 1 0) planar configuration is the lowest energy structure for the charged V_3 defect. The FFC and (1 1 0) planar configurations of V_3 in Si can be seen in Fig. 6 of Ref. [3]. V_3 in the planar configuration gives rise to two acceptor levels at 0.36 and 0.46 eV below the conduction band edge (E_c) and to two donor levels at 0.19 and 0.11 eV above the valence band edge (E_v), while in the FFC configuration it has only an acceptor level at E_c–0.075 eV [3,12]. Five signals observed in the DLTS spectra of electron-irradiated Si diodes were associated with charge carrier emission from the above levels. It should be mentioned that storage of the irradiated Si samples for a few weeks at room temperature or shorter anneals in the temperature range 50–100 °C resulted in the transformation of V_3 from the (1 1 0) planar configuration into the most stable FFC one, while the defect could be restored to the metastable planar configuration by an application of forward bias injection with a current density in the range 10–15 A/cm^2 for 10–20 min at about 300 K. The above transformations between the FFC and (1 1 0) planar configurations were found to be fully reversible in both the electron-irradiated n- and p-type Si samples [3,12].

It was found in Refs. [3, 12] that 30-min isochronal annealing of the irradiated p^+–n and n^+–p diodes in the temperature range 200–275 °C resulted in the disappearance of the levels due to V_3 and to the correlated appearance of a defect with two acceptor levels at 0.34 and 0.455 eV below E_c and to two donor levels at 0.23 and 0.12 eV above E_v. It was suggested that the disappearance of V_3 upon annealing at temperatures above 200 °C could be associated with its diffusion and interaction with interstitial oxygen, the most abundant impurity in the samples studied. The above four levels were tentatively assigned to the energy levels of the V_3O complex. Further arguments for the suggested model and level assignments are given in the present study.

Fig. 1 shows changes in concentrations of the V_2 and V_3 defects upon 30 min isochronal annealing of an electron-irradiated epi-Si p^+–n diode. Changes in concentrations of the defects, which emerge simultaneously with the disappearance of V_2 and V_3, are also shown. Apparently, the annealing behaviors of the V_2 and V_3 centers are very similar. There is strong experimental evidence that the elimination of divacancies in oxygen-rich Si samples is associated with their interaction with oxygen atoms and results in the formation of a V_2O defect [5,13]. Taking into account similar structures and electronic properties of V_2 and the V_3 defect in the (1 1 0) planar configuration, it can be suggested that the disappearance of V_3 upon isochronal annealing, similar to that of divacancies, is associated with the diffusion of trivacancies and their interaction with interstitial oxygen atoms.

Further results supporting the suggested annealing scenario have been obtained from isothermal annealing studies of the irradiated diodes in the temperature range 230–270 °C. It has been found that the kinetics of the decay of both the V_2 and V_3

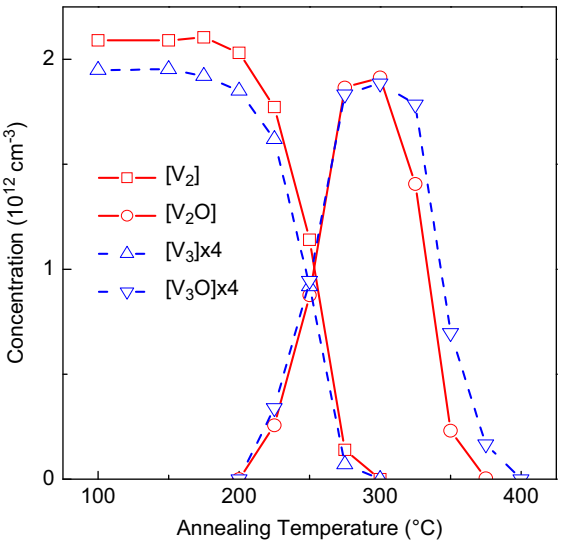

Fig. 1. Changes in concentrations of the V_2- and V_3-related defects upon 30 min isochronal annealing of an electron-irradiated epi-Si p^+–n diode. Concentrations of the V_3-related defects are multiplied by 4. (For interpretation of the references to color in this figure legend, the reader is referred to the web version of this article.)

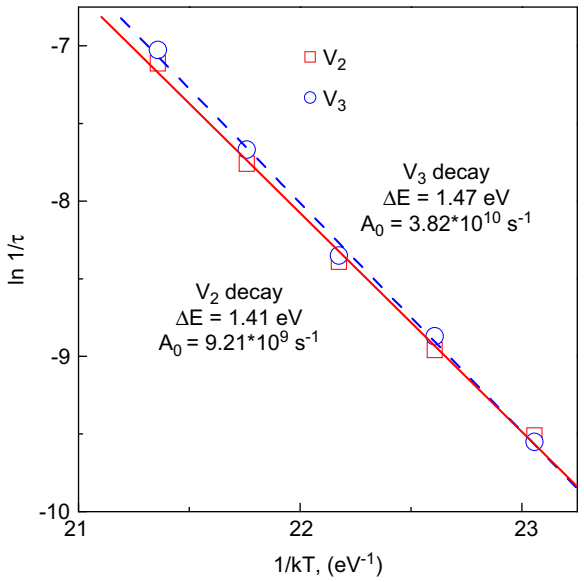

Fig. 2. Arrhenius plots of the elimination rate constants for the divacancy and trivacancy in electron-irradiated n-type epi-Si. (For interpretation of the references to color in this figure legend, the reader is referred to the web version of this article.)

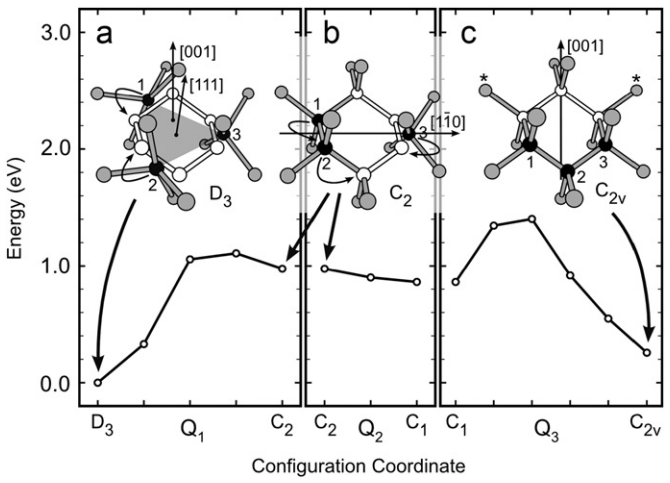

Fig. 3. Configuration coordinate model for the V_3 migration path. The process is divided into three steps represented by coordinates Q_1, Q_2 and Q_3 shown in (a), (b) and (c), respectively. Ticks in the configuration coordinate axes represent intermediate structures. Several configurations are identified by their point group symmetry, namely D_3, C_2, C_1 and C_{2v} structures. Relevant atomic models are also shown, whose atom coloring is explained in the text.

defects upon isothermal annealing in the above temperature range are described well by mono-exponential functions with very similar rate constants. The kinetics of the anti-correlated formation of the V_2O and V_3O defects are also found to be nearly coincident. It should be mentioned here that the decay kinetics of the V_2 and V_3 and appearance kinetics of the V_2O and V_3O centers have been compared within the same diodes. An evidence of the involvement of oxygen into the reactions resulting in elimination of V_2 and V_3 has been obtained from a comparison of the reaction rates in epi-Si and Cz-Si diodes. The rates of the above reactions are found to be twice as fast as in Cz-Si diodes, where $[O_i]$ is 7.5×10^{17} cm^{-3}, compared to those in epi-p-Si diodes ($[O_i]\approx4\times10^{17}$ cm^{-3}).

Fig. 2 shows Arrhenius plots of elimination rate constants for the V_2 and V_3 defects in electron-irradiated n-type epi-Si. The activation energy and pre-exponential factor of the process for V_2 have been found to be 1.41 ± 0.05 eV and 9.2×10^9 s^{-1}, while the values for V_3 have been determined as 1.47 ± 0.04 eV and 3.8×10^{10} s^{-1}.

3.2. Modeling results

One can envisage two solutions for the migration of neutral V_3, namely, (i) a *thermally activated* mechanism where the FFC $V_3(D_3)$ form is the ground state (starting and end structures of the migration step), or (ii) an *enhanced* mechanism, where $V_3(D_3)$ is immobile but somehow (e.g., by getting energy from free carriers) it converts into PHR $V_3(C_{2v})$ form, which is the mobile species. Hence, like V_2 in Si [14], $V_3(C_{2v})$ could then migrate by means of a mechanism where end-atoms move across the vacant space.

In the latter mechanism, the C_{2v} form, shown in Fig. 3(c), is the starting and end structure of the migration process. Upon relaxation of 9 intermediate structures connected by an elastic coupling constraint (elastic band), we found that the saddle point is a structure with C_{2h} symmetry, where one of the Si atoms labeled with a '*' in Fig. 3(c) has been displaced to the bond-center site, at mid-way to the furthest vacant site. The $V_3(C_{2v})\rightarrow V_3(C_{2h})\rightarrow V_3(C_{2v})$ migration barrier is calculated as $E_m=2.18$ eV, which is too high to account for the experimental observations.

For mechanism (i) the $V_3(D_3)$ structure represents both starting and end points of the migration process. Usually, in vacancy related migration mechanisms, breaking/formation of bonds take place. Here vacancy-related radicals, reconstructed and twisted bonds play a major role, owed to their reactivity and readiness to be saturated. These are usually the chemical driving forces for diffusion and their identification may solve much of the problem. However, for extended defects such as $V_3(D_3)$, a diffusion mechanism involves collective atomic motion, the search for such paths requires sampling of large portions of the phase space, and therefore the use of computationally intensive methods such as molecular dynamics (MD) are often employed. Unfortunately, MD calculations are intractable if one wants to adequately account for the long-range strain fields that are produced by small vacancy clusters, which means using supercells or clusters with hundreds of host atoms [15,16]. Our strategy was then to hypothesize that a consecutive transformation between D_3 and C_{2v} structures could result in a mechanism with a migration barrier compatible with the kinetics measurements.

Several paths were investigated by setting specific intermediate structures to be relaxed by the NEB method. The minimum energy path comprises three main steps, which are shown in Fig. 3(a), (b) and (c) with respective configuration coordinates Q_1, Q_2 and Q_3, respectively. In the structures depicted, gray, black and white balls represent Si atoms that hardly move along the path, Si atoms that are significantly displaced along the path, and lattice sites from where Si atoms have been displaced, respectively. During the first step (see in Fig. 3(a)), a pair of Si atoms among those numbered from 1 to 3 dimerize by taking the place of two nearest neighboring vacant sites. The barrier surmounted is 1.11 eV high, and the structure attained has C_2 symmetry with a principal axis along the $\langle 1\,1\,0\rangle$ direction. The $V_3(C_2)$ structure has two equivalent three-fold coordinated Si radicals (Si_1 and Si_2 atoms in Fig. 3(b)) that are responsible for the highest occupied (symmetric) and lowest unoccupied (anti-symmetric) dangling bond states. Step 2 comprises a distortion of the Si_1–Si_2 dimer, resulting in a relaxation of 0.11 eV from $V_3(C_2)$ to a $V_3(C_1)$ triclinic structure. This effect is similar to that in Si(0 0 1) surface dimers, where electron transfer between symmetric radicals results in tilted dimer reconstructions with a $\sim$0.16 eV relaxation gain per Si pair [17]. In step 3, the tilted Si_1–Si_2 dimer makes a correlated jump to the next available vacant sites (see Fig. 3(b)), and this results in a spontaneous formation of the Si_2–Si_3 bond (Fig. 3(c)). This is the limiting step of the whole mechanism with a $E_m=1.40$ eV high barrier, which is in very good agreement with

the experimental value from the isochronal annealing studies reported above.

According to the defect alignment in Fig. 3(a), the first step has three possible solutions (ending with [1 $\bar{1}$ 0], [1 0 $\bar{1}$] and [0 $\bar{1}$ 1] $V_3(C_2)$ aligned structures, respectively). Further, after taking steps 2 and 3, each of these three orientations can transform to two $V_3(C_{2v})$ alignments. This means that the mechanism $Q_1 \rightarrow Q_2 \rightarrow Q_3$ provides a connecting path between a [1 1 1]-aligned $V_3(D_3)$ complex and the full family of $\langle 1\,1\,0 \rangle$-$V_3(C_{2v})$ aligned defects. The symmetry of the problem allows us to envisage six possible $V_3(C_{2v}) \rightarrow V_3(D_3)$ (backward) two-fold transformations in order to attain the full family of equivalent $\langle 1\,1\,1 \rangle$-aligned $V_3(D_3)$ complexes as well. Hence, the proposed migration is also a reorientation mechanism, where the $V_3(D_3)$ complex *jumps* between neighboring $\langle 1\,1\,1 \rangle$ hexagonal rings.

4. Conclusions

Our density functional modeling studies show that in-plane motion of Si atoms across the PHR $V_3(C_{2v})$ vacancy has a high migration (2.18 eV) barrier. This is not only considerably higher that the experimental value obtained for diffusion of V_3 (1.47 eV), but also much higher than previous theoretical estimates (1.36 eV) for the migration barrier of V_2 in Si [14]. So, we propose that V_3 migration occurs by means of consecutive transformations between $V_3(D_3)$ and $V_3(C_{2v})$ forms. This mechanism shows a barrier $E_m = 1.40$ eV, in very good agreement with the experimental value.

Acknowledgments

We would like to thank the Engineering and Physical Research Council (EPSRC—UK) and BRFFR (Belarus) for financial support of this work.

References

[1] D.V. Makhov, L.J. Lewis, Phys. Rev. Lett. 92 (2004) 255504-(1-4).
[2] D.A. Abdulmalik, P.G. Coleman, Phys. Rev. Lett. 100 (2008) 095503-(1-4).
[3] V.P. Markevich, A.R. Peaker, S.B. Lastovskii, L.I. Murin, J. Coutinho, V.J.B. Torres, P.R. Briddon, L. Dobaczewski, E.V. Monakhov, B.G. Svensson, Phys. Rev. B 80 (2009) 235207-(1-7).
[4] J.L. Hastings, S.K. Estreicher, Phys. Rev. B 56 (1997) 10215.
[5] M. Mikelsen, E.V. Monakhov, G. Alfieri, B.S. Avset, B.G. Svensson, Phys. Rev. B 72 (2005) 195207-(1-6).
[6] M.J. Rayson, P.R. Briddon, Comp. Phys. Commun. 178 (2008) 128.
[7] J.P. Perdew, Y. Wang, Phys. Rev. B 45 (1992) 13244.
[8] C. Hartwigsen, S. Goedecker, J. Hutter, Phys. Rev. B 58 (1998) 3641.
[9] G. Henkelman, B.P. Uberuaga, H. Jónsson, J. Chem. Phys. 113 (2000) 9901.
[10] A. Carvalho, R. Jones, M. Sanati, S.K. Estreicher, J. Coutinho, P.R. Briddon, Phys. Rev. B 73 (2006) 245210-(1-7).
[11] A. Carvalho, R. Jones, C. Janke, J.P. Goss, P.R. Briddon, J. Coutinho, S. Öberg, Phys. Rev. Lett. 99 (2007) 175502-(1-4).
[12] V.P. Markevich, A.R. Peaker, B. Hamilton, S.B. Lastovskii, L.I. Murin, J. Coutinho, V.J.B. Torres, L. Dobaczewski, B.G. Svensson, Phys. Status Solidi A 208 (2009) 568.
[13] V.P. Markevich, A.R. Peaker, S.B. Lastovskii, L.I. Murin, J.L. Lindström, J. Phys.: Condens. Matter 15 (2003) S2779.
[14] G.S. Hwang, W.A. Goddard III, Phys. Rev. B 65 (2002) 233205-(1-3).
[15] S. Öğüt, J.R. Chelikowsky, Phys. Rev. Lett. 83 (1999) 3852.
[16] T.E.M. Staab, A. Sieck, M. Haugk, M.J. Puska, T. Frauenheim, H.S. Leipner, Phys. Rev. B 65 (2002) 115210-(1-11).
[17] D.J. Chadi, Phys. Rev. Lett. 43 (1979) 43.